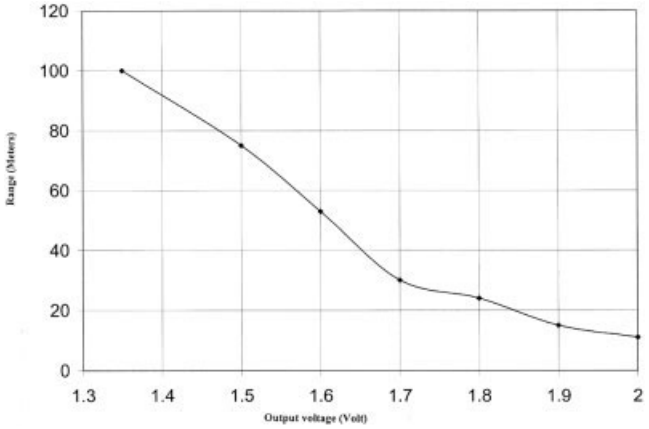

Figure 5 Relationship between the noise voltage and RKE system range

measurements at the receiver output. The curve shown reveals the relationship between the noise-voltage level and the system range (the system provides for more than 97% successful transmission over 360° around the car).

5. CONCLUSION

A measurement procedure for signal and noise estimation of an RKE system in a vehicle using an active antenna and an RF receiver has been proposed. Using this procedure, the signal and noise of an RKE module in a car in a noisy environment can be measured at the required range. Range estimation based on the test data, according to the described test procedure, was confirmed by laboratory experiments with a remote-control module. We can conclude that such a measurement procedure will be useful in helping to design a properly operating RKE system.

REFERENCES

1. F.L. Dacus, Design of short range radio systems, Microwaves RF 40 (2001), 73–80.
2. A. Bensky, Short-range wireless communications, LLH Technology Publishing, 2000.
3. J. Salter, Specifying UHF active antennas and calculating system performance, Research & Development British Broadcasting Corporation, White Paper 066, 2003.
4. A. Bensky, Range estimation for short-range event transmission systems, RF Design (2002), 30–38.
5. G.W. Milne, E.J. Jansen, J.J. Roux, J. Koekemoer, and P.A. Kotze, EMC and RFI problems and solutions on the SUNSAT micro-satellite, South African Symp Commun Signal Processing, Cape Town, South Africa, 1998, pp 293–298.
6. B. Al-Khateeb, V. Rabinovich, and B. Oakley, An active receiving antenna for short-range wireless automotive communication, Microwave Opt Technol Lett 44 (2004), 200–205.

INVESTIGATION OF MICROSTRIPLIKE MODE SUPPRESSION IN UC-PBG FW-CBCPW BY USING AN ELECTRO-OPTIC NEAR-FIELD CHARACTERIZATION

K.-H. Oh,[1] H.-J. Song,[1] S. Moon,[1] T.-Y. Kim,[1] G. Mudhana,[1] W. B. Kim,[2] D.-Y. Kim,[1] and J.-I. Song[1]
[1] Department of Information and Communications
Gwangju Institute of Science and Technology
1 Oryong-dong, Buk-gu
Gwangju, 500-712, Korea
[2] Department of Electrical Engineering
Songwon College
199-1 Gwangchun-dong Seo-gu
Gwangju, Korea

Received 13 April 2005

ABSTRACT: *Near-field patterns of uniplanar compact photonic bandgap (UC-PBG) and non-UCPBG finite-width conductor-backed coplanar waveguides (FW-CBCPWs) are characterized using an electro-optic near-field mapping system. This system is very effective in visually showing the role of the UC-PBG structure in the suppression of microstriplike (MSL) modes in the FW-CBCPWs.* © 2005 Wiley Periodicals, Inc. Microwave Opt Technol Lett 47: 119–122, 2005; Published online in Wiley InterScience (www.interscience.wiley.com). DOI 10.1002/mop.21098

Key words: *electro-optic near-field characterization; FW-CBCPW; MSL mode; UC-PBG*

INTRODUCTION

Circuits based on coplanar waveguides (CPWs) offer advantages, including an easy parallel and series access of passive and active components without using via holes, as compared to those based on microstrip lines. However, special care must be taken to avoid the effects of undesired propagation modes when broadband performance is required. In finite-width conductor-backed coplanar waveguides (FW-CBCPWs), there are two dominant modes, CPW and microstriplike (MSL) modes, having no cutoff frequencies, as illustrated in Figure 1 [1, 2]. Thus, unless certain mode-suppression techniques are employed, undesirable MSL modes, including higher-order resonance modes, may be excited and propagate along the structures, resulting in circuit-performance deterioration. The resonance peaks observed in the *S*-parameter measurements of the FW-CBCPWs are related to the excitation of extra higher-order modes (in the form of the MSL mode), which are supported by the 2D resonator formed by finite-width side-ground plates on both sides of the center signal-strip [2]. The conventional method to suppress the MSL mode in FW-CBCPWs was to use via holes to connect the two side-ground plates to the bottom-ground plate [3]. However, this method complicates the fabrication process. A photonic bandgap (PBG) structure, called an uniplanar compact photonic bandgap (UC-PBG) structure, has been reported to efficiently suppress the MSL mode in FW-CBCPWs and thus improves the transmission characteristics without losing the advantages of CPWs [4, 5]. Verification of the MSL mode suppression utilizing the novel PBG structure in FW-CBCPWs was carried out by using computer-aided simulations or *S*-parameter measurements. However, the computer-aided simulations provide field distributions obtained from theoretical analysis of idealized microwave circuit structures, and the *S*-parameter measurements can provide only an indirect indication of MSL mode suppression inferred from the difference in *S*-parameters of the conventional non-UC-PBG and

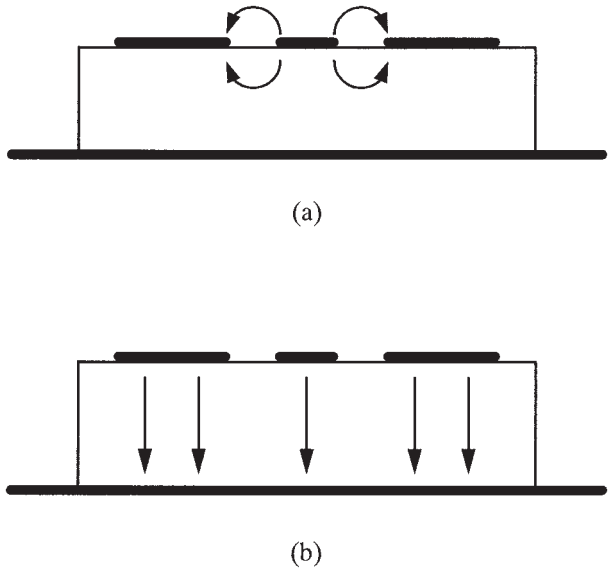

Figure 1 Dominant modes in FW-CBCPW: (a) CPW mode; (b) MSL mode

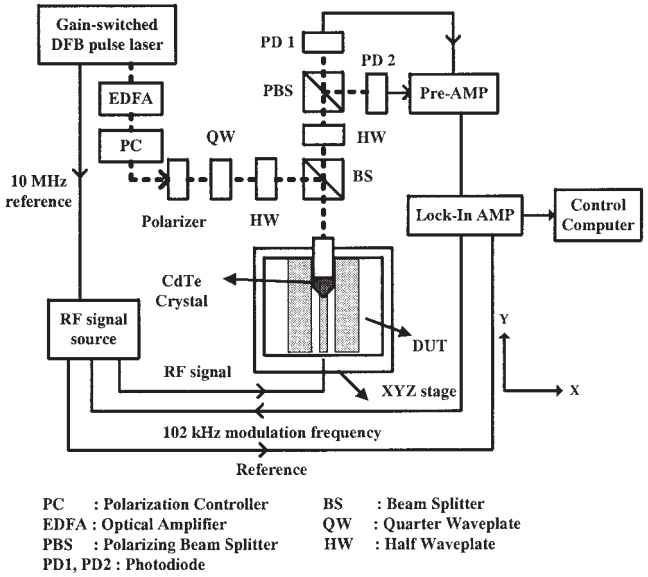

Figure 3 Schematic diagram of the electro-optic field-mapping system

UC-PBG FW-CBCPWs. Recently, an electro-optic field-mapping technique was successfully applied for experimentally characterizing a patch antenna by visually showing near-field radiation patterns [6].

In this paper, we investigate the role of the UC-PBG structure in suppression of the parasitic MSL mode in the UC-PBG FW-CBCPW by using an electro-optic near-field mapping system based on a gain-switched distributed feedback (DFB) pulsed laser and a CdTe electro-optic crystal.

EXPERIMENTS AND RESULTS

Non-UC-PBG and UC-PBG FW-CBCPWs, shown in Figure 2, were fabricated on an FR4 substrate having thickness of 1.6 mm, dielectric constant of 4.3, and 43-μm-thick Cu metallizations on both sides of the substrate. The length of the FW-CBCPWs is 40 mm and the widths of the center signal-strip and the side-ground plates are 2.5 and 8 mm, respectively, with a slot width of 0.97 mm. The dimensions of the two FW-CBCPWs are the same, except for UC-PBG patterns on the side-ground plates in the case of the UC-PBG FW-CBCPW. This UC-PBG structure, realized with metal pads etched in the ground plane connected by narrow lines to form a distributed *LC* network, has a very compact PBG lattice and a distinctive stop-band, and is known to be effective in reducing leakage of MSL modes to the side-ground plates [4]. The UC-PBG pattern on the side-ground plates was designed to have a stop band around the X-band using the well-known scaling technique [4, 5].

The schematic diagram of the electro-optic field mapping system is shown in Figure 3. The system uses a gain-switched DFB pulsed laser that is very compact, convenient, and inexpensive, as compared to the conventionally used phase-stabilized Ti:Sapphire laser [6]. The optical beam from the phase-stabilized gain-switched DFB pulsed laser has a pulse width of 16 ps and a repetition rate of 10 MHz. A 100-cut CdTe crystal, that has a high electro-optic coefficient and transparency to the wavelength of the DFB laser, was used to measure the normal component (z component) of RF electric fields. The crystal's tip thickness and diameter are 100 and 500 μm, respectively, and it is attached to a

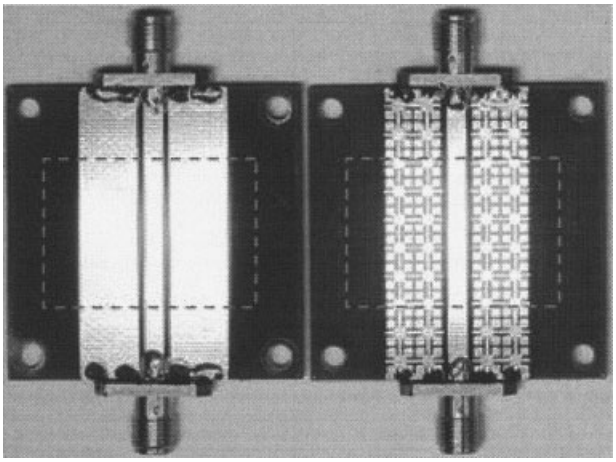

Figure 2 Fabricated FW-CBCPWs: Non-UC-PBG (left) and UC-PBG (right). The dotted area (20 × 30 mm) was measured

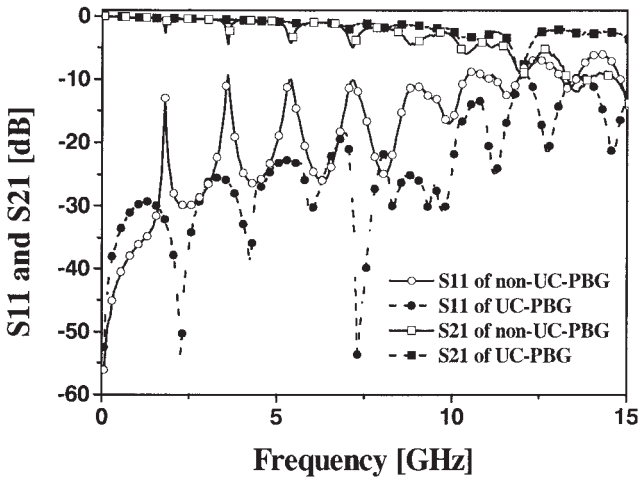

Figure 4 Measured *S*-parameters of the non-UC-PBG and UC-PBG FW-CBCPWs

TABLE 1 Measured and Calculated Resonant Frequencies of the non-UC-PBG FW-CBCFW

Resonance Number	Measured Resonant Frequencies [GHz]	Calculated Resonant Frequencies [GHz]
1	1.800	1.808
2	3.600	3.617
3	5.400	5.425
4	7.150	7.234

conical-type fused silica for easy handling. The output power of the RF signal source was approximately 15 dBm and the output port of the FW-CBCPW was terminated with a 50Ω termination. The measurements were done over the scanning area of 20 × 30 mm^2 highlighted in Figure 2, with 0.25-mm resolution in close proximity to the top surface of FW-CBCPWs.

Figure 4 shows the measured scattering parameters (S_{11} and S_{21}) of the non-UC-PBG and UC-PBG FW-CBCPWs. The non-UC-PBG FW-CBCPW showed periodic resonant frequencies due to resonant MSL modes. The resonant frequencies of the MSL modes in the non-UC-PBG FW-CBCPW can be obtained quantitatively by solving the following equation [2]:

$$\beta_{MSL} l = n\pi, \tag{1}$$

where β_{MSL} is the propagation constant of the dominant or higher-order MSL modes, l is the length of the side-ground plate (in the y-direction, as shown in Fig. 3), and n is the integer. Table 1 shows the measured and calculated resonant frequencies of the non-UC-PBG FW-CBCPW. The UC-PBG FW-CBCPW showed improved transmission characteristics, which were pronounced around the X-band frequency where the stop-band of the UC-PBG is located. Figure 5 shows transmission characteristics of the UC-PBG FW-CBCPW and a conventional microstrip line having the width (2.5 mm) of the line identical to that of the center signal-strip of the UC-PBG FW-CBCPW. The difference in transmission characteristics indicates that the CPW mode is the dominant mode in the UC-PBG FW-CBCPW.

Figure 6 shows the normalized electric-field distribution of the non-UC-PBG and UC-PBG FW-CBCPWs at frequencies of 1.8, 3.6, 5.4, and 7.2 GHz. As can be seen in Figure 6(a), in the non-UC-PBG FW-CBCPW the electric field not only exists along

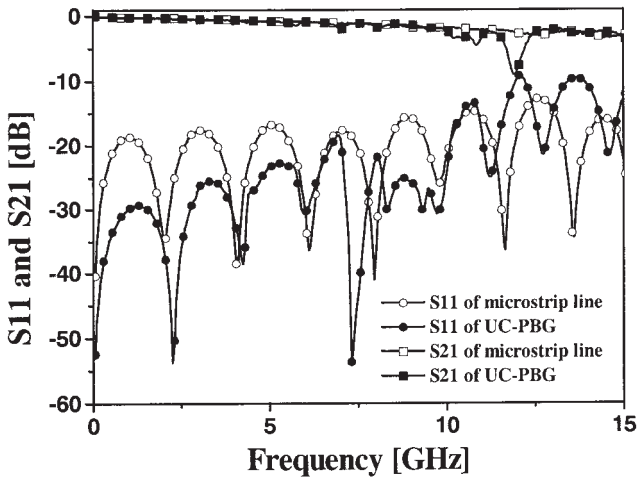

Figure 5 Measured S-parameters of the conventional microstrip line and the UC-PBG FW-CBCPW

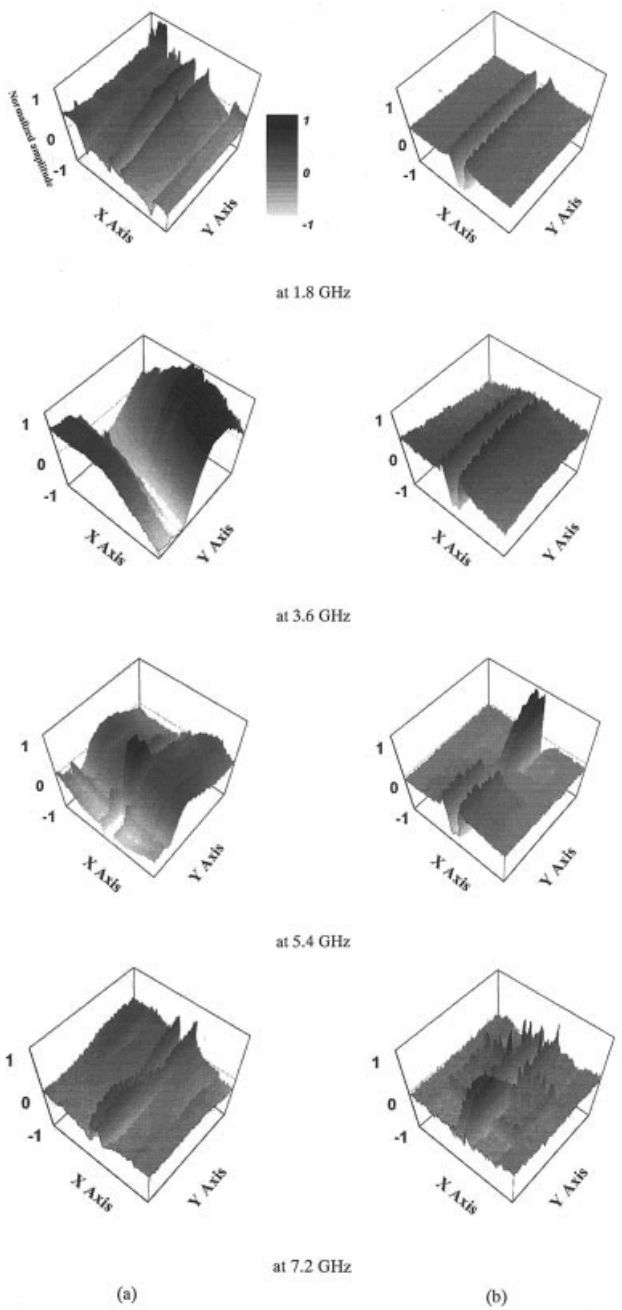

Figure 6 Measured near-field patterns of the non-UC-PBG and UC-PBG FW-CBCPWs at resonant frequencies of 1.8, 3.6, 5.4, and 7.2 GHz for (a) the non-UC-PBG FW-CBCPW and (b) the UC-PBG FW-CBCPW

the slot regions but also spreads over the entire side-ground plates, indicating that CPW and resonant MSL modes coexist. Also, note that the measured field patterns show resonant MSL modes in longitudinal (y) direction, as predicted by Eq. (1). On the other hand, as can be seen in Figure 6(b), the electric field in the UC-PBG FW-CBCPW is concentrated along the slot regions, showing that the CPW mode is dominant and the resonant MSL modes are effectively suppressed by using the UC-PBG structure.

CONCLUSION

The role of the UC-PBG pattern in suppression of parasitic MSL modes in UC-PBG FW-CBCPWs was investigated visually by using an electro-optic near-field mapping system based on a gain-

switched distributed feedback (DFB) pulsed laser and a CdTe electro-optic crystal. The results showed the potential of the electro-optic near-field mapping system for use in characterizing novel planar microwave-integrated circuits.

ACKNOWLEDGMENTS

The authors would like to thank Dr. Tadao Nagatsuma and Dr. Ai-Ichiro Sasaki of NTT Microsystem Integration Laboratories for their helpful comments on our study. This work was supported, in part, by the ITRC (Ministry of Information and Communications)–CHOAN and Fusion Tech (MOST) programs.

REFERENCES

1. C.-C. Tien, C.-K.C. Tzuang, S.T. Peng, and C.-C. Chang, Transmission characteristics of finite-width conductor-backed coplanar waveguide, IEEE Trans Microwave Theory Tech 41 (1993), 1616–1624.
2. W.-T. Lo, C.-K.C. Tzuang, S.-T. Peng, C.-C. Tien, C.-C. Chang, and J.W. Huang, Resonant phenomena in conductor-backed coplanar waveguides (CBCPW's), IEEE Trans Microwave Theory Tech 41 (1993), 2099–2108.
3. M. Yu, R. Vahldieck, and J. Huang, Comparing coax launcher and wafer probe excitation for 10-mil conductor-backed CPW with via holes and airbridges, IEEE MTT-Symp Dig 2 (1993), 705–708.
4. F.-R. Yang, K.-P. Ma, Y. Qian, and T. Itoh, A uniplanar compact photonic-bandgap (UC-PBG) structure and its applications for microwave circuits, IEEE Trans Microwave Theory Tech 47 (1999), 1509–1514.
5. L.C. Kretly, L.C. Marangoni, and A. Tavora, Photonic band gap metallic 2D matrix applied to microstrip CPW lines to operate at Ka band, IEEE MTT-Symp IMOC Dig 1 (2001), 435–438.
6. K. Yang, G. David, J.-G. Yook, I. Papapolymerou, L.P.B. Katehi, and J.F. Whitaker, Electrooptic mapping and finite-element modeling of the near-field pattern of a microstrip patch antenna, IEEE Trans Microwave Theory Tech 48 (2000), 288–294.

A CONTINUOUS-WAVE MILLIMETER WAVE GENERATED FROM OPTICAL SIGNALS BY APPLYING OPTICAL TECHNOLOGY FOR OPTICAL-TO-RADIO SYSTEMS

K. H. Park
Optical Communication System Lab
Dept. of Optical Engineering
Sejong University
98, Gunjadong, Kwangjin-ku
Seoul 143-747, Korea

Received 10 April 2005

ABSTRACT: *A 50-GHz continuous-wave millimeter wave was generated from optical signals by applying optical technology for optical-to-radio systems. The generated MMW signals were radiated in a millimeter waveguide and detected by a detector. The spectral linewidth of the MMW signals was less than 1 kHz, and the power fluctuation of the MMW was less than 1.5 dB over the 30–50-GHz range.* © 2005 Wiley Periodicals, Inc. Microwave Opt Technol Lett 47: 122–123, 2005; Published online in Wiley InterScience (www.interscience.wiley.com). DOI 10.1002/mop.21099

Key words: *optical-to-radio systems; mobile communications; millimeter-wave; optical and millimeter-wave technology*

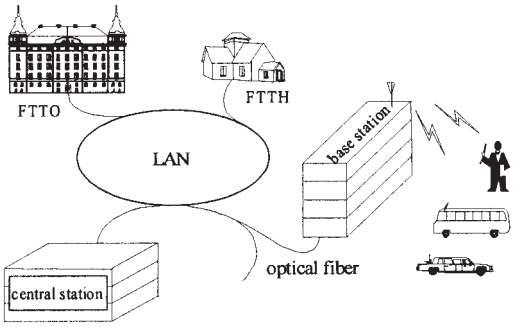

Figure 1 Distribution network of optical and MMW signals

INTRODUCTION

Millimeter waves (MMWs) have been used as a favorable means of data transmission for wireless and mobile communications. However, the available frequency range of MMWs has been limited, according to the development of new communication systems and the incremental increase of subscribers. Researchers have proposed a MMW region between 30–70 GHz so that a high antenna gain can be more easily provided in new communication-frequency bands in order to overcome this problem [1]. They have also concentrated on radio-on-fiber (ROF) systems, which transmit MMW signals over optical fibers [2]. However, this method leads to a large loss of MMW signals, and the MMW-transmission distance is too short. Therefore, this paper proposes optical-to-radio (O/R) systems, which generate MMW signals by using optical signals transmitted over optical fibers to the antennas set up on the roof of a building, the ceiling of an office or home, and so on (Fig. 1).

O/R systems, which generate MMWs in the local area by using the optical signals transmitted from the central station connected to the optical networks to the base station, are a reliable transmission method for the transmission of large-capacity information and for delivering broad-bandwidth service. Accordingly, the development of technology which generates a coherent continuous-wave (CW) MMW with a narrow spectral bandwidth at room temperature is desirable for O/R systems. Generating MMW signals from optical signals using optical technology is a very attractive technology for future broadband wireless and ubiquitous communication systems, particularly operating at several tens of GHz [3, 4]. MMW signals are generated by optical signals and radiated from the antenna. This technology enables broadband operation, has low signal loss, and is immune to signal-distribution interference and exposure to unfavorable environmental conditions, including sun, snow, wind, and rain.

Generating coherent sub-MMWs and MMWs by using difference-frequency generation (DFG) has also been investigated with optically nonlinear materials [5, 6]. Using the DFG method, one can obtain the desired MMW frequency easily by controlling the frequency spacing of the input optical signals. However, pico- or femto-second optical pulses have been used in most studies so as to ensure to high temporal coherence of generated MMW. Therefore, a very high optical-peak-power is required for the experiment. Dual-mode distributed feedback lasers (DFBs) have been developed for the optical generation of MMW for broad bandwidth mobile communication and radio-on-fiber systems. However, so far, their spectral linewidths have been too large for use in these systems. Furthermore, detecting MMWs by using a photodiode leads to the rapid decrease of signal power at high frequencies due to the typical characteristics of a photodiode. Also, this method provides only a narrow bandwidth of several GHz for communication systems.